Tree Physiology 26, 257–273

A mathematical model linking tree sap flow dynamics to daily stem diameter fluctuations and radial stem growth

KATHY STEPPE,[1,2] DIRK J. W. DE PAUW,[3] RAOUL LEMEUR[1] and PETER A. VANROLLEGHEM[3]

[1] *Department of Applied Ecology and Environmental Biology, Laboratory of Plant Ecology, Ghent University, Coupure links 653, B-9000 Ghent, Belgium*

[2] *Corresponding author (kathy.steppe@ugent.be)*

[3] *Department of Applied Mathematics, Biometrics and Process Control (BIOMATH), Ghent University, Coupure links 653, B-9000 Ghent, Belgium*

Received May 6, 2005; accepted June 11, 2005; published online December 15, 2005

Summary To date, models for simulating sap flow dynamics in individual trees with a direct link to stem diameter variation include only the diameter fluctuation driven by a change in stem water storage. This paper reports results obtained with a comprehensive flow and storage model using whole-tree leaf transpiration as the only input variable. The model includes radial stem growth based on Lockhart's equation for irreversible cell expansion. It was demonstrated that including growth is essential to obtaining good simulation results. To model sap flow dynamics, capacitance of storage tissues was assumed either constant (i.e., electrical analogue approach) or variable and dependent on the water content of the respective storage tissue (i.e., hydraulic system approach). These approaches resulted in different shapes for the desorption curve used to calculate the capacitance of storage tissues. Comparison of these methods allowed detection of specific differences in model simulation of sap flow at the stem base (F(stem)) and stem diameter variation (D). Sensitivity analysis was performed to select a limited subset of identifiable parameters driving most of the variability in model predictions of F(stem) and D. Both the electrical analogue and the hydraulic system approach for the flow and storage model were successfully calibrated and validated for the case of a young beech tree (*Fagus sylvatica* L.). Use of an objective model selection criterion revealed that the flow and storage model based on the electrical analogue approach yielded better predictions.

Keywords: beech, capacitance, desorption curve, identifiability, Lockhart's equation, model selection, parameter estimation, sensitivity analysis, stem diameter variation, water relations, water storage.

Introduction

A correct mathematical translation of water flow behavior in plants and trees has fascinated plant physiologists for many years. In a first attempt to describe water transport in plants mathematically, van den Honert (1948) proposed a simple Ohm's law analogue model. For this model to hold, the plant must be regarded as a simple rigid tube where steady-state water flow conditions occur. However, the assumption of steady-state flow conditions in plants, and particularly in trees, is unrealistic, as is documented by the extensive literature on time lags between water loss by leaf transpiration and water uptake by roots (e.g., Schulze et al. 1985, Goldstein et al. 1998, Steppe et al. 2002, Steppe and Lemeur 2004). The time lags can be explained only by the use of internally stored water. This internal reservoir can be depleted and subsequently replenished on a daily basis, causing the stem diameter to shrink and swell accordingly (e.g., Herzog et al. 1995, Tatarinov and Èermák 1999, Zweifel et al. 2000, Zweifel and Häsler 2001, Steppe 2004).

Adjustment of van den Honert's model to accommodate dynamic water flow in plants led initially to the development of dynamic models, based on either a hydraulic system (e.g., Edwards et al. 1986, Tyree 1988, Zweifel et al. 2001) or on an electrical analogue (e.g., Landsberg et al. 1976, Lhomme et al. 2001). Such models usually account for the storage of water in the stem, branches and leaves by inclusion of one or more hydraulic plant capacitances (see reviews by Jarvis et al. 1981 and Hunt et al. 1991).

Recently, dynamic models for water flow in individual trees have also taken into account the link between the change in stem water storage and the daily variation in whole stem diameter (e.g., Zweifel and Häsler 2001, Zweifel et al. 2001). These models attribute stem diameter variation to the imbalance between water loss and water uptake. However, it is clear that in addition to daily diameter fluctuation caused by water storage changes, stem diameter variation also depends on growth processes. Water flow into cells leads to irreversible changes in cell volume if it is accompanied by cell wall extension. This physiological process can be described by Lockhart's equation (1965).

Growth phenomena based on Lockhart's equation have not yet been incorporated in dynamic flow and storage models. On the contrary, growth effects on stem diameter fluctuations are

often eliminated from the measured data by subtracting linear growth from the stem diameter variation (Sevanto et al. 2002). It is not known if this linear trend line represents actual stem growth, or if the actual daily fluctuations in stem diameter can be detected this way. To answer these questions and to gain more insight into the underlying mechanisms driving stem diameter variation, growth effects need to be included in dynamic water flow and water storage models.

The purpose of the present study was to develop a dynamic flow and storage model that includes both stem growth and the daily stem diameter fluctuation resulting from changes in stem water storage. In addition, two approaches to calculate the capacitance (C) of storage tissues were compared. The dynamic flow and storage model is referred to as HydGro (i.e., hydraulic system approach) when capacitance is variable and depends on the water content of the storage tissue, or as RCGro (i.e., electrical analogue approach) when capacitance is constant. Both models are driven by whole-tree leaf transpiration. After sensitivity analysis for selection of a subset of identifiable model parameters, both HydGro and RCGro were calibrated and validated for the case of a 2-year-old beech tree (*Fagus sylvatica* L.). Model predictions are compared for changes in stem diameter variation (combined effect of water storage and stem growth) and the sap flow rate at the stem base. We also identify specific differences between HydGro and RCGro and assess the better model based on an objective criterion.

Materials and methods

Plant material

The flow and storage model was calibrated and validated for a 2-year-old beech tree (*Fagus sylvatica*). The young tree was planted in a container (0.4 m diameter × 0.4 m in height) and placed in a growth room of the Laboratory of Plant Ecology (Ghent University, Belgium). The container was filled with a mixture of 60% silt loam soil (i.e., 38.6% sand, 50.8% silt and 11.6% clay) and 40% peat. The tree was about 1.5 m high and had a stem diameter at the soil surface of 17.6 mm.

Photosynthetically active radiation (PAR) and air temperature in the growth room were measured above the tree with a quantum sensor (Li-190S, Li-Cor, Lincoln, NE) and thermocouples (Thermocouple T, Omega, Netherlands), respectively. Relative humidity of the air was monitored with an RH sensor (HIH-3605-A, Honeywell) and fluctuated freely depending on irradiance, air temperature and the transpiration rate of the tree. Soil water potential in the container was measured with a miniature type electronic tensiometer (SWT5, Delta-T devices, U.K.) and was maintained above –20 kPa.

Physiological measurements

Transpiration rate (E) and sap flow at the stem base (F(stem)) were continuously measured with Dynagage sap flow sensors based on the heat balance principle. The sensors were installed according to the instructions manual (van Bavel and van Bavel 1990). Based on the close correspondence between leaf transpiration rates measured with a "branch-bag–ADC H_2O Infrared Gas Analysis" system and sap flow rates in the supporting branch of the tree (Steppe 2004, Steppe and Lemeur 2004), the diurnal courses of sap flow measured (SGA5, Dynamax, USA) in a selected second-order branch (diameter = 4.1 mm) at the top of the young tree were used as a surrogate for the diurnal courses of E. Hence, leaf water storage can be neglected in the case of the well-watered young tree. With leaf area as a scaling factor, sap flow rates at the second-order branch level were upscaled to whole-tree leaf transpiration. Diurnal courses of F(stem) were measured (SGB16, Dynamex) at the base of the stem (diameter = 17.6 mm). To record diurnal changes in branch and stem temperature for correction of the sap flow calculations for the heat storage term (Grime et al. 1995), a small thermocouple was placed at the center of the sensor heater between the heater and the surface of the tree segment.

Variations in stem diameter were detected with a linear variable displacement transducer (LVDT; LBB 375-PA-100 and transducer bridge 8C-35, Schaevitz, USA). The LVDT was attached to the stem with a custom-made stainless steel holder. Control runs demonstrated that no temperature corrections were required for the LVDT support system, nor for the thermal expansion of the xylem of the beech tree (Steppe 2004).

All sensor outputs were recorded every 10 s and 5-min means were stored in a computer connected to the data acquisition system (HP 34970A, Hewlett Packard, USA).

Model description

In the flow and storage model, transpiration is the only input variable, because water transport in the tree is linked to stem diameter variation for given daily courses of whole-tree leaf transpiration. Stem diameter variation is assumed to result from daily changes in water storage as well as from growth. Thus, the model consists of: (1) a submodel for calculating dynamic water transport; and (2) a submodel for predicting stem diameter variation. In the first submodel, a distinction is made depending on the way the capacitance of storage tissues is calculated.

Concept of the dynamic water transport submodel

The flow and storage model (Figure 1) consists of two types of elements: storage compartments and flow path sections. Two internal water storage compartments are defined: the crown storage pool located at the top of the model tree, representing mainly first-order branches without leaves and the elastic stem storage pool, which includes the living part of the stem bark. The crown storage pool includes branches and leaves when E is actually measured instead of using branch sap flow as a surrogate. The soil is considered as a non-limiting external water storage pool. The experimental conditions chosen allowed us to ignore the change in xylem water content due to cavitation. The storage compartments are connected by two flow paths: F(crown) connects the two internal water storage pools and

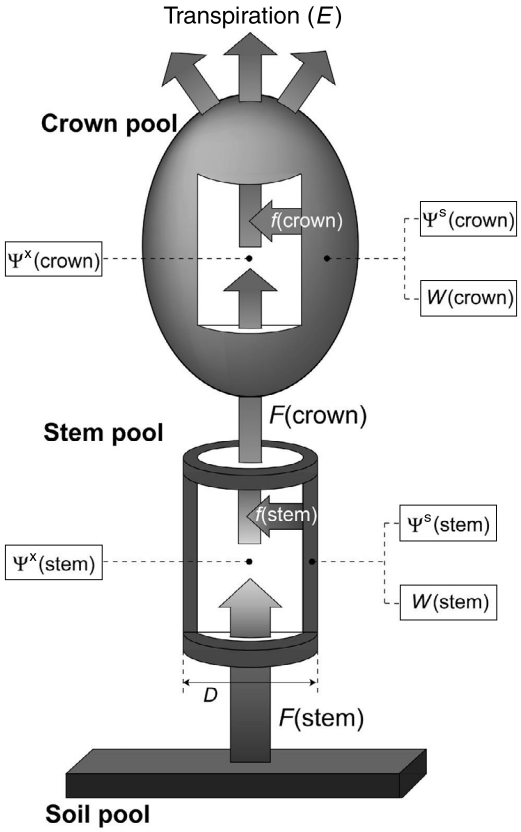

Figure 1. Schematic of the single-tree flow and storage model. The model consists of two internal water storage compartments (pools for crown and stem), one external water source (soil pool) and two flow paths (F(stem) and F(crown)). The model is driven by transpiration (E). Flow rates into and out of the stem (i.e., bark) and the crown storage compartments are represented by f(stem) and f(crown), respectively. Abbreviations: Ψ^x(pool) = water potential in the indicated xylem compartment; Ψ^s(pool) = water potential in the indicated storage compartment; W(stem) and W(crown) = water content of stem and crown storage pool, respectively; and D = stem diameter.

F(stem) connects the stem storage pool with the soil. Transpiration rate in the crown top starts a chain of events throughout the tree. It affects the xylem water potential of the crown (Ψ^x(crown)). In response to the decrease in Ψ^x(crown), a water potential difference develops in the xylem that induces water flow in the upper part of the tree (F(crown)). In addition to xylem water flow, water from the crown storage pool can contribute to the transpiration stream, because of the hydraulic connection between stored water and xylem water (Zweifel et al. 2000, 2001, Zweifel and Häsler 2001, Génard et al. 2001, Steppe and Lemeur 2004). As water is withdrawn from the crown storage compartment, the water content (W(crown)) decreases and the water potential (Ψ^s(crown)) is lowered. The tension developed in the xylem by transpiration is further transmitted through the stem of the tree toward the roots resulting in two new water potential differences: one in the xylem between stem and roots, and one between the xylem and the stem storage pool. Whereas the water potential difference in the xylem induces a vertical water flow in the lower flow section of the model tree (F(stem)), the water potential difference between xylem and bark causes a radial water flow from the stem storage compartment toward the xylem. As a result, the water content of the living part of the stem bark (W(stem)) decreases and, consequently, stem diameter (D) shrinks. The water potential of the stem storage pool (Ψ^s(stem)) is lowered as the stem tissue contracts and this will proceed until the difference between xylem water potential of the stem (Ψ^x(stem)) and Ψ^s(stem) is zero.

To translate the phenomenon of dynamic water transport in trees into mathematical equations, a choice is generally made between a hydraulic system approach or an electrical circuit analogue. In this study, both approaches are included and compared. The major difference between these approaches is the way the capacitance of storage tissues is calculated (see below). Model design is based on the diagrams depicted in Figure 2. Lists of all model variables and parameters (including units and definitions) are presented in Tables 1 and 2.

Model assumptions The model comprises two sequential flow paths (i.e., F(stem) and F(crown)), with F(stem) set equal to F(roots) (Figure 2) because no important time lags could be detected between stem and root sap flow in the young tree (Steppe 2004). We assumed that the two flow paths have an equal flow resistance (R^x(stem) = R^x(crown) = R^x) (cf. Zweifel et al. 2001) and that the exchange resistance between the xylem and the storage compartment of the stem and the crown is equal (R^s(stem) = R^s(crown) = R^s). We also set the water potential of the xylem root compartment equal to the soil water potential (Ψ^x(roots) = Ψ(soil)). This approximation is justified because the model aims mainly to simulate the physiological processes within the tree (i.e., from the xylem root compartment and higher). Furthermore, all simulations of time series were started at the end of the night when equal values of water potentials prevail in the soil-plant continuum, because E is zero (Nobel 1999).

Basic flow equations Depending on the model approach used, the mathematical description of the water transport in the xylem flow path sections can be expressed by Darcy's law (hydraulic system approach, Figure 2a), or derived from Ohm's law (electrical analogue approach, Figure 2b):

$$F(\text{stem}) = -\frac{\Psi^x(\text{stem}) - \Psi^x(\text{roots})}{R^x} \quad (1)$$

$$F(\text{crown}) = -\frac{\Psi^x(\text{crown}) - \Psi^x(\text{stem})}{R^x} \quad (2)$$

Water potentials in the xylem compartments are thereby entirely determined by their negative pressure potential component, because the osmotic potential of the xylem sap is negligible (Jones 1992, Nobel 1999). Besides vertical water transport, internally stored water can contribute to the daily transpiration stream because of the hydraulic connection be-

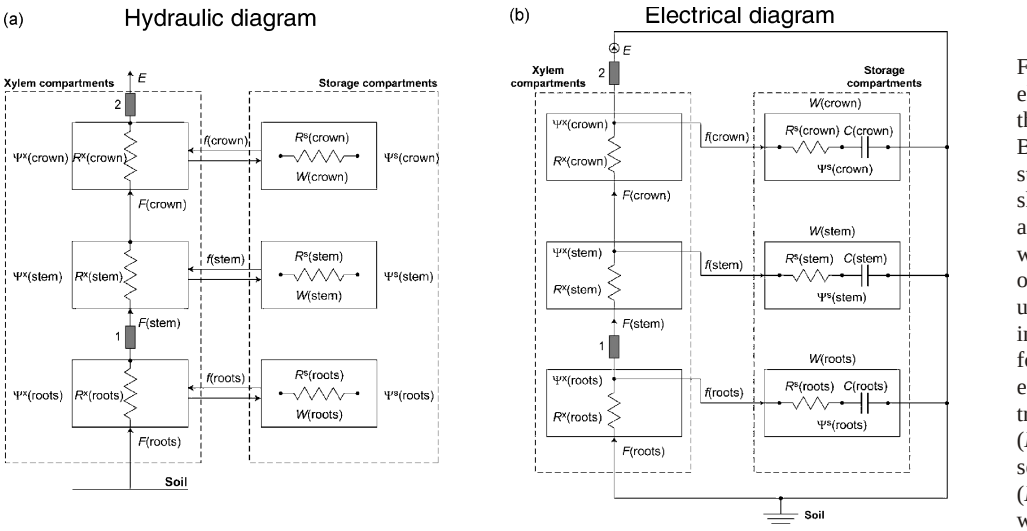

Figure 2. Hydraulic (a) and electrical (b) representation of the water transport submodel. Both the xylem (x) and the storage (s) compartments are shown. The pools are defined as crown, stem (equivalent with bark) and roots. Positions of the physiological sensors used during measurements are indicated: 1 = sap flow sensor for sap flow F(stem) and linear variable displacement transducer for stem diameter (D) variation; and 2 = sap flow sensor for transpiration rate (E). Abbreviations: W(pool) = water content stored in the storage compartment of a pool; Ψ^s(pool) = water potential in a storage compartment; Ψ^x(pool) = water potential in a xylem compartment; f(pool) = water exchange between the xylem and the storage compartment of a pool; F(pool) = water flow into a xylem compartment; R^s(pool) = exchange resistance between a xylem and a storage compartment; R^x(pool) = flow resistance in a xylem compartment; and C(pool) = capacitance of the storage compartment of a pool.

tween xylem and storage pools (Simonneau et al. 1993, Zweifel et al. 2000, 2001, Zweifel and Häsler 2001, Génard et al. 2001, Steppe 2004, Steppe and Lemeur 2004). This contribution depends on the magnitude of the hydraulic exchange resistance (R^s) that must be overcome when water flows from the storage compartments toward the xylem to equilibrate the imbalance between water supply and demand during the day (Lhomme et al. 2001). Water flow to or from the storage pool f(pool) can be expressed as:

$$f(\text{pool}) = \frac{\Psi^x(\text{pool}) - \Psi^s(\text{pool})}{R^s} \quad (3)$$

This flow rate is equivalent to the first derivative expressing the change in the water content of the storage pool:

$$f(\text{pool}) = \frac{dW(\text{pool})}{dt} \quad (4)$$

Values of f(pool) are negative when water is withdrawn from the storage pool and positive when the storage pool is refilled. Combining xylem flow and storage flow, the flow rates out of the xylem compartments can be derived from either the water mass balance equation (hydraulic approach, Figure 2a), or from Kirchhoff's electrical current law, whereby the flow rates represent the currents flowing in the electrical network (electrical analogue approach, Figure 2b):

$$E = F(\text{crown}) - f(\text{crown}) \quad (5)$$

$$F(\text{crown}) = F(\text{stem}) - f(\text{stem}) \quad (6)$$

Table 1. Symbol, unit and description of the model variables. Pools are defined as crown, stem and roots (Figure 2). Superscripts x and s refer to the xylem and the storage compartment, respectively.

Symbol	Unit	Description
A	m^2	Surface area of the virtual membrane separating the stem storage compartment from the xylem compartment
d^s	m	Thickness of storage compartment
D	m	Outer diameter of stem segment
D_i	m	Inner diameter of stem segment
f(pool)	mg s^{-1}	Water exchange between the xylem and the storage compartment of a pool
F(pool)	mg s^{-1}	Water flow in a xylem compartment
V^s	m^3	Volume of storage compartment
V(stem)	m^3	Volume of water in stem storage compartment
W(pool)	mg	Water content stored in storage compartment
Ψ^s(pool)	MPa	Total water potential in a storage compartment
Ψ^x(pool)	MPa	Total water potential in a xylem compartment
Ψ^s_π	MPa	Osmotic component of the water potential in storage compartment
Ψ^s_p	MPa	Pressure component of the water potential in storage compartment

Table 2. Symbol, unit and description of the model parameters.

Symbol	Unit	Description
a	m	Allometric parameter
b	m^{-1}	Allometric parameter
C(pool)	mg MPa^{-1}	Capacitance of storage compartment of a pool
k_1(pool)	mg	Amount of stored water at the inflection point of the desorption curve
k_2(pool)	unitless	Index for rate of change of Ψ^s(pool) at the inflection point of the desorption curve
l	m	Length of stem segment
L	m MPa^{-1} s^{-1}	Radial hydraulic conductivity of the virtual membrane separating the stem storage compartment from the xylem compartment
R^s	MPa s mg^{-1}	Exchange resistance between a xylem and a storage compartment
R^x	MPa s mg^{-1}	Flow resistance in a xylem compartment
β	unitless	Empirical parameter for the initial condition of the pressure potential of the storage compartment (Ψ^s_p)
ε	MPa	Bulk elastic modulus of living tissue in relation to reversible dimensional changes (water storage)
ε_0	m^{-1}	Proportionality constant
ϕ	MPa^{-1} s^{-1}	Extensibility of cell walls in relation to non-reversible dimensional changes (growth of tissue)
ρ_w	mg m^{-3}	Density of water
Γ	MPa	Critical value for the pressure component (Ψ^s_p) which must be exceeded to produce (positive) growth in the storage compartment
σ_r	unitless	Reflection coefficient of the virtual membrane to solutes in the xylem sap
Ψ^x(roots)	MPa	Xylem water potential in roots
Ψ^s_{min}(pool)	MPa	Lowest water potential of the storage compartment when W(pool) $\rightarrow 0$
$\Psi^x(\Psi^s_p = 0)$	MPa	Water potential of stem xylem for which the zero pressure potential in the storage compartment is reached

Derived flow equations Combining Equations 2, 4 and 5, the water exchange rate between the xylem and the storage compartment of the crown can be rewritten as:

$$\frac{dW(\text{crown})}{dt} = \frac{\Psi^x(\text{stem}) - \Psi^x(\text{crown})}{R^x} - E \tag{7}$$

Substituting the equation expressing the xylem water potential:

$$\Psi^x(\text{pool}) = \frac{dW(\text{pool})}{dt} R^s + \Psi^s(\text{pool}) \tag{8}$$

for Ψ^x(crown) in Equation 7 leads to:

$$\frac{dW(\text{crown})}{dt} = \frac{\Psi^x(\text{stem}) - \Psi^s(\text{crown}) - R^x E}{R^x + R^s} \tag{9}$$

In a similar way, the water exchange rate between the xylem and the stem storage compartment can be deduced:

$$\frac{dW(\text{stem})}{dt} = \frac{\Psi^x(\text{roots}) - 2\Psi^s(\text{stem}) + \Psi^x(\text{crown})}{R^x + 2R^s} \tag{10}$$

Rewriting Equation 10 in terms of storage water potentials yields:

$$\frac{dW(\text{stem})}{dt} = \frac{R^x + R^s}{(R^x + R^s)(R^x + 2R^s) - (R^s)^2} \left(\begin{array}{l} \Psi^x(\text{roots}) + \left(\dfrac{R^s}{R^x + R^s} - 2 \right) \Psi^s(\text{stem}) + \left(1 - \dfrac{R^s}{R^x + R^s} \right) \\ \Psi^s(\text{crown}) - \dfrac{R^x R^s E}{R^x + R^s} \end{array} \right) \tag{11}$$

Equations for desorption curve and hydraulic capacitance Solving Equation 11 involves an expression for calculating the water potential of the storage pools. In this respect, the hydraulic system approach differs from the electrical analogue. In the hydraulic system approach, the desorption curve, as defined by Zweifel et al. (2000, 2001), directly relates the total water potential of a storage compartment to its water content (Figure 3):

$$\Psi^s(\text{pool}) = \frac{\Psi^s_{min}(\text{pool})}{1 + \exp\left(\dfrac{W(\text{pool}) - k_1(\text{pool})}{k_2(\text{pool})} \right)} \tag{12}$$

In accordance with Zweifel et al. (2001), the same function is used for both crown and stem storage compartments, but with different parameter values for Ψ^s_{min}(pool), k_1(pool) and k_2(pool).

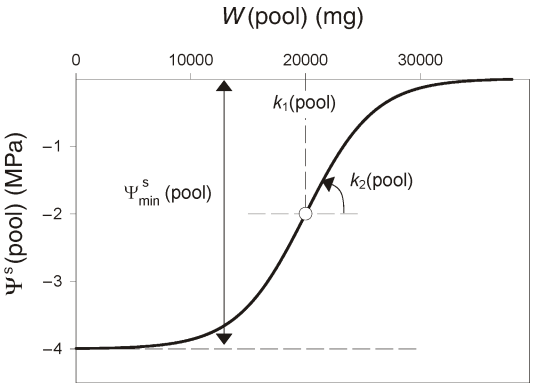

Figure 3. Idealized desorption curve and the parameters of Equation 12. Abbreviations: W(pool) = available water content of storage tissue; Ψ^s(pool) = water potential of storage tissue; k_1(pool) = amount of stored water at the inflection point; k_2(pool) = index for rate of change of Ψ^s(pool) at the inflection point; and Ψ^s_{min}(pool) = minimum water potential of storage compartment.

In the electrical analogue approach, the function that relates the total water potential of the storage compartment to its water content is given by:

$$\Psi^s(\text{pool}) = \Psi^x(\text{roots}) + \frac{W(\text{pool})}{C(\text{pool})} \quad (13)$$

This function can be interpreted as a desorption curve; however, in contrast to the one proposed by Zweifel et al. (2000, 2001), it now represents a straight line with a slope equal to the inverse of the capacitance. Application of the laws for electrical networks leads to Equation 13, where the flow between the xylem and the storage compartment of a pool is given by the first derivative of its water content (Equation 4). In this equation, f(pool) represents the current flowing in the electrical circuit (Figure 2b), whereas W(pool) corresponds to the total charge on the capacitor. The capacitance of the storage tissue C(pool) can also be defined as the ratio of the change in the amount of water (volume or mass) present in the storage tissue to the change in water potential of the tissue (e.g., Jarvis et al. 1981, Hunt et al. 1991, Jones 1992):

$$C(\text{pool}) = \frac{\mathrm{d}W(\text{pool})}{\mathrm{d}\Psi(\text{pool})} \quad (14)$$

Based on this definition, the value of C(pool) can be determined as the inverse of the slope of the curve expressing the relationship between Ψ^s(pool) and W(pool). Thus, the capacitance is variable for the hydraulic system approach (Figure 3), whereas it remains fixed for the electrical analogue approach.

Concept of the stem diameter variation submodel

Model assumptions Daily stem diameter fluctuation is caused by changes in the hydration of the stem. Irreversible increase in stem diameter is caused by growth. It is well known that water flow into growing cells can lead to an irreversible change in cell volume. According to the widely used Lockhart model (1965), cell expansion is driven largely by turgor pressure (i.e., positive pressure potential), which irreversibly deforms the cell wall as the cell compartment expands. The expansion requires turgor above a threshold value before irreversible deformation begins. Based on Lockhart's equation, Génard et al. (2001) developed a biophysical model for stem and root diameter variation in woody plants that offers a basis for integrating water storage compartments and diameter growth into a dynamic water transport model. After restructuring the model of Génard et al. (2001), by making water flow between the xylem and the stem storage compartment a linking variable between the water transport submodel on the one hand and the stem diameter variation submodel on the other hand, parts of the model of Génard et al. (2001) were incorporated in the dynamic flow and storage model.

The stem diameter variation submodel is designed to simulate stem diameter variation resulting from both changes in water storage (stem diameter fluctuation) and growth. For this purpose, the stem is modeled as two coaxial cylinders separated by a "virtual" membrane (Figure 4). We assumed that the xylem forms a continuous rigid cylinder bound by an outer ring composed of various extensible tissues (i.e., bark composed of phloem and cambium) (cf. Génard et al. 2001). The external cylinder is considered as the stem storage compartment and can swell and shrink in response to radial water flow from the xylem. The "virtual" membrane represents the membranes and cell walls of several cell layers participating in apoplastic and symplastic water flow between the overall system of extensible tissue ("single cell") and the rigid xylem system.

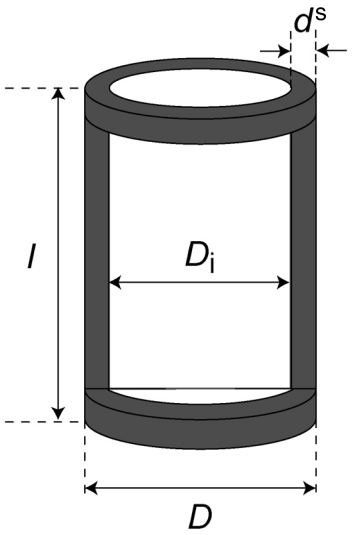

Figure 4. Geometric representation of a stem segment. A stem with diameter D comprises two coaxial cylinders of length l, separated by a membrane. Mature xylem is represented by the inner cylinder of diameter D_i. Extensible tissues of the bark are represented by the external cylindrical layer of thickness d^s.

Basic equations for stem geometry The stem geometry proposed by Génard et al. (2001) is used in the present submodel. The thickness of the storage compartment (d^s) is equal to (Figure 4):

$$d^s = \frac{D - D_i}{2} \tag{15}$$

where D and D_i are the outer and inner diameter of the stem segment.

The volume of the storage compartment (V^s) can be written as:

$$V^s = \frac{\pi l}{4}\left(D^2 - D_i^2\right) \tag{16}$$

where l is stem segment length.

Assuming d^s is much smaller compared to D_i, Equation 16 can be rewritten as:

$$V^s \cong \pi d^s D_i l \tag{17}$$

The approximation made in Equation 17 is necessary to simplify further analyses of the stem diameter variation submodel. Génard et al. (2001) showed that the error resulting from this simplified function is less than 10%. Additional assumptions and equations in the submodel included the following.

Relationship between the thickness of the storage compartment (d^s) and the outer stem diameter (D):

$$d^s = a\left(1 - e^{-bD}\right) \tag{18}$$

where a and b are parameters. This empirical relationship is taken from Génard et al. (2001) and is based on the observation that the thickness of extensible tissues increases with the diameter of the organ (Huguet 1985). Génard et al. (2001) measured the thickness of extensible tissues on three peach cultivars and by a nonlinear regression procedure estimated the values of a and b as 2.968×10^{-3} m and 32 m^{-1}, respectively. We used the same relationship and parameter values for the young beech tree.

The relationship between the change in pressure potential of the storage compartment and the relative change of the storage compartment volume (Nobel 1999) is:

$$\frac{d\Psi_p^s}{dt} = \frac{\varepsilon}{V^s}\frac{dV^s}{dt} \tag{19}$$

Elastic modulus (ε) is proportional (ε_0) to the product of the outer diameter and the pressure potential:

$$\varepsilon = \varepsilon_0 D \Psi_p^s \tag{20}$$

The elastic modulus increases with pressure potential and cell size (Tyree and Jarvis 1982) and reaches an asymptotic value for both high pressure potentials and cell sizes. However, to minimize the number of model parameters and in accordance with Génard et al. (2001), we assumed a linear relationship between ε and pressure potential and the outer diameter of the stem.

The relative volume change of the storage compartment (plastic growth) depends on the pressure potential when a critical value (Γ) is exceeded (ϕ is a proportionality constant called cell wall extensibility; see below):

$$\frac{1}{V^s}\frac{dV^s}{dt} = \phi\left(\Psi_p^s - \Gamma\right) \qquad \text{when } \Psi_p^s > \Gamma \tag{21}$$

$$\frac{1}{V^s}\frac{dV^s}{dt} = 0 \qquad \text{when } \Psi_p^s \le \Gamma \tag{22}$$

Derived equations for the stem diameter variation We assumed that variation in stem diameter D per unit time is the result of an elastic (el) and a growth (gr) component:

$$\frac{dD}{dt} = \left(\frac{dD}{dt}\right)_{el} + \left(\frac{dD}{dt}\right)_{gr} \tag{23}$$

Stem diameter variation resulting from elastic changes (first term in Equation 23) can be calculated from Equation 15 using Equations 17, 19 and 20; thereby assuming that the inner diameter of the stem does not change:

$$\left(\frac{dD}{dt}\right)_{el} = 2\frac{dd^s}{dt} = \frac{2d^s}{V^s}\frac{dV^s}{dt} = \frac{2d^s}{\varepsilon}\frac{d\Psi_p^s}{dt} = \frac{2d^s}{\varepsilon_0 D \Psi_p^s}\frac{d\Psi_p^s}{dt} \tag{24}$$

The elastic change in stem diameter occurs because a small change in volume produces a change in pressure potential (Equation 19). The amount of this change depends on the bulk elastic modulus ε that expresses the elasticity of cell walls, i.e., a larger elasticity of cell walls is explained by a smaller value of the elastic modulus (Lambers et al. 1998, Nobel 1999). The dependency of ε on the pressure potential and the outer stem diameter is defined by Equation 20.

Stem diameter variation resulting from growth (second term in Equation 23) can be expressed as an algebraic equivalence:

$$\left(\frac{dD}{dt}\right)_{gr} = \frac{dD}{dd^s}\left(\frac{dd^s}{dt}\right)_{gr} \tag{25}$$

The quest to calculate dD/dd^s led to the introduction of Equation 18, from which it can be derived:

$$\left(\frac{dD}{dd^s}\right) = \frac{1}{b(a - d^s)} \tag{26}$$

Besides Equation 26, stem diameter variation caused by

growth involves an expression for the change in thickness d^s. For this purpose, D_i was considered to be constant compared with d^s for plastic growth on a small time scale (e.g., hourly basis); plastic growth being defined as permanent deformation leading to dimensional changes in stem diameter components. The model most widely used for plastic growth has been developed by Lockhart (1965) and is described by both Equations 21 and 22. Thus, plastic growth is a pressure potential driven process, controlled by the physical properties of the primary cell wall (Lambers et al. 1998), and can be written using Equations 17 and 21:

$$\left(\frac{\mathrm{d}d^s}{\mathrm{d}t}\right)_{gr} = \frac{d^s}{V^s}\left(\frac{\mathrm{d}V^s}{\mathrm{d}t}\right)_{gr} = d^s\phi(\Psi_p^s - \Gamma) \tag{27}$$

Combining Equations 25, 26 and 27, stem diameter variation due to growth is obtained as:

$$\left(\frac{\mathrm{d}D}{\mathrm{d}t}\right)_{gr} = \frac{d^s\phi}{b(a-d^s)}(\Psi_p^s - \Gamma) \text{ when } \Psi_p^s > \Gamma \tag{28}$$

$$\left(\frac{\mathrm{d}D}{\mathrm{d}t}\right)_{gr} = 0 \qquad \text{when } \Psi_p^s \le \Gamma \tag{29}$$

Stem diameter variation due to both elastic changes and growth can then be written as:

$$\left(\frac{\mathrm{d}D}{\mathrm{d}t}\right) = \frac{2d^s}{\varepsilon_0 D\Psi_p^s}\frac{\mathrm{d}\Psi_p^s}{\mathrm{d}t} + \frac{d^s\phi}{b(a-d^s)}(\Psi_p^s - \Gamma) \qquad \text{when } \Psi_p^s > \Gamma \tag{30}$$

$$\left(\frac{\mathrm{d}D}{\mathrm{d}t}\right) = \frac{2d^s}{\varepsilon_0 D\Psi_p^s}\frac{\mathrm{d}\Psi_p^s}{\mathrm{d}t} \qquad \text{when } \Psi_p^s \le \Gamma \tag{31}$$

Furthermore, d^s and D_i are computed as:

$$\frac{\mathrm{d}d^s}{\mathrm{d}t} = abe^{(-bD)}\frac{\mathrm{d}D}{\mathrm{d}t} \tag{32}$$

$$\frac{\mathrm{d}D_i}{\mathrm{d}t} = \frac{\mathrm{d}D}{\mathrm{d}t} - 2\frac{\mathrm{d}d^s}{\mathrm{d}t} \tag{33}$$

Equation for the pressure potential component Incorporation of growth in the submodel for stem diameter variation (solving Equations 30 and 31) needs an expression for the pressure potential Ψ_p^s in the stem storage compartment. From the assumption that the change in water volume caused by water exchange between the xylem and the stem storage compartment is equal to the volume change of the storage compartment:

$$\frac{\mathrm{d}V(\text{stem})}{\mathrm{d}t} = \frac{\mathrm{d}V^s}{\mathrm{d}t} \tag{34}$$

and using the conversion from gravimetric weight (W) change to a change in water volume (V):

$$\frac{\mathrm{d}V(\text{stem})}{\mathrm{d}t} = \frac{1}{\rho_w}\frac{\mathrm{d}W(\text{stem})}{\mathrm{d}t} \tag{35}$$

it can be deduced, using Equation 19 and 20 and after rearrangement, that the change in pressure potential results from the flow of water in and out of the stem storage compartment:

$$\frac{\mathrm{d}\Psi_p^s}{\mathrm{d}t} = \frac{\varepsilon_0 D\Psi_p^s}{\rho_w V^s}\frac{\mathrm{d}W(\text{stem})}{\mathrm{d}t} \tag{36}$$

Equation 36 establishes the direct link between the water transport submodel and the submodel for stem diameter variation. Once the pressure component in the storage compartment (s) is known, the osmotic component can be found from the total water potential:

$$\Psi_\pi^s = \Psi^s - \Psi_p^s \tag{37}$$

Equation for the exchange resistance The flow of water between the xylem and the storage compartment in the stem can be derived from non-equilibrium thermodynamics (Katchalsky and Curran 1965):

$$\frac{\mathrm{d}V(\text{stem})}{\mathrm{d}t} = AL\begin{pmatrix}\Psi_p^x(\text{stem}) + \sigma_r\Psi_\pi^x(\text{stem}) - \\ \Psi_p^s(\text{stem}) - \sigma_r\Psi_\pi^s(\text{stem})\end{pmatrix} \tag{38}$$

where A is surface area of the virtual membrane separating the xylem from the stem storage compartment (= $\pi D_i l$) and L is radial hydraulic conductivity of this membrane. For the "single cell" model approach, a tissue reflection coefficient σ_r of 1 could be assumed. The "virtual" membrane represents several layers that lead to possible symplastic or apoplastic water flow, or both. The reflection coefficient of the apoplast is usually close to 0, whereas along the symplastic path the presence of the membrane leads to a reflection coefficient close to 1 (Steudle 2000). The overall tissue reflection will then be between 0 and 1. Because for the "single cell" approach most of the water has to cross the cell membrane (Génard et al. 2001), a reflection coefficient of 1 can be adopted. With this assumption, Equation 38 reduces to:

$$\frac{\mathrm{d}V(\text{stem})}{\mathrm{d}t} = AL\left(\Psi^x(\text{stem}) - \Psi^s(\text{stem})\right) \tag{39}$$

Substituting Equation 35 for $\mathrm{d}V(\text{stem})/\mathrm{d}t$ yields:

$$\frac{\mathrm{d}W(\text{stem})}{\mathrm{d}t} = \rho_w AL\left(\Psi^x(\text{stem}) - \Psi^s(\text{stem})\right) \tag{40}$$

Identification of Equation 3 from Equation 40 reveals that hydraulic exchange resistance, R^s, is inversely proportional to radial hydraulic conductivity L:

$$R^s = \frac{1}{\rho_w AL} \tag{41}$$

Model implementation

The flow and storage model, schematically depicted in Figure 5, consists of a set of algebraic and differential equations that must be solved numerically. The complete set of equations for each model approach was implemented in the (C++) MSL-EXEC language of the modeling and simulation software package WEST (Hemmis NV, Kortrijk, Belgium). Detailed information on WEST is given by Vanhooren et al. (2003). After compilation of the (C++) MSL-EXEC code, a compiled library is obtained and loaded in the experimentation environment of WEST. This environment allows simulation, optimization, sensitivity analysis and optimal experimental design. Henceforth, the compiled flow and storage model is referred to as HydGro or RCGro when the hydraulic system approach or the electrical analogue approach is used in the water transport submodel, respectively.

Sensitivity analysis

Model calibration will be successful only if all model parameters are identifiable. To be identifiable, a parameter must fulfil two conditions: (1) the model output must be sufficiently sensitive to changes in the parameter value and (2) the parameters must not be highly correlated (Brun et al. 2002, Dochain and Vanrolleghem 2001). Because both HydGro and RCGro comprise a large set of parameters (17 and 13, respectively; see Table 2), it might be expected that not all parameters are identifiable. Sensitivity analysis was therefore performed to select a subset of identifiable parameters for final estimation.

To examine the first condition for a parameter to be identifiable, a sensitivity measure δ^{meas} similar to that of Brun et al. (2002) was used. Such a measure allows assessment of the relative importance of individual parameters for the model output and can be used to rank the parameters. In this respect, the sensitivity $S(y_i)$ was calculated as follows:

$$S(y_i) = \frac{y_i(\theta + \Delta\theta) - y_i(\theta - \Delta\theta)}{2y_i(\theta)} 100 \tag{42}$$

where y_i is the output of the model variable at a certain time i, θ is the parameter value and $\Delta\theta$ is the perturbation of the parameter. The perturbation factor was chosen to be 10% of the parameter value. Based on the sensitivity $S(y_i)$, the sensitivity measure δ^{meas} was defined as:

$$\delta^{meas} = \frac{1}{N}\sum_{i=1}^{N}\left|S(y_i)\right| \tag{43}$$

where N is number of sensitivity values along the time axis. The value of δ^{meas} measures the mean sensitivity of the model output resulting from a change in parameter θ. A high δ^{meas} means that the value of θ has an important influence on the simulated model result. The parameters driving most of the variability in the model outputs F(stem) and D were identified. These two output variables were chosen as being qualified for model calibration because they were obtained by independent methods.

The selection of the dominant subset of parameters was complemented with an analysis of parameter correlation. The sensitivities (Equation 42) were plotted and visually compared. Parameters were assumed to be highly correlated when their sensitivities were nearly proportional (Dochain and Vanrolleghem 2001). In the case of a highly correlated and highly ranked parameter pair, one of the parameters was given an assumed value which facilitated estimation of the other. Such a procedure finally led to a subset of dominant parameters (i.e., k_2(stem), k_2(crown), k_1(stem), k_1(crown), C(stem), C(crown), R^x, β, ϕ, L), all of which were identifiable.

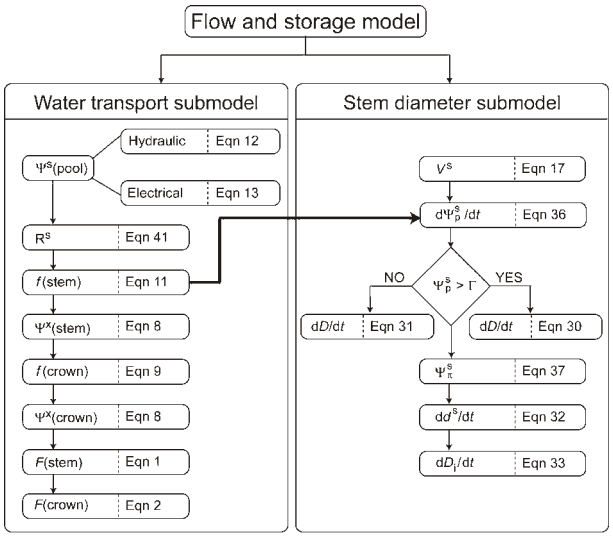

Figure 5. Schematic of the flow and storage model linking sap flow dynamics in a tree to daily stem diameter fluctuations and stem growth.

Initial conditions and parameters

The remaining non-identifiable model parameters were set at an assumed value (either taken from literature or directly measured or calculated). Xylem root water potential Ψ^x(roots) was approximated from soil water potential measurements made during the night preceding collection of the data set used for simulation, as −0.0086 MPa. The Ψ^s_{min}(pool) values for crown and stem were set at −4 and −3 MPa, respectively (cf. Bréda et al. 1993, Cochard et al. 1996, 1999, Zweifel et al. 2001, Raftoyannis and Radoglou 2002, Larcher 2003). Values of the allometric parameters a and b in Equation 18 were those reported by Génard et al. (2001) (i.e., 2.968×10^{-3} m and 32 m^{-1}, respectively). Different values of the wall-yielding threshold pressure Γ have been observed, ranging from 0.1 to 0.9 MPa (Green et al. 1971, Green and Cummins 1974, Bradford and Hsiao 1982, Hsiao and Xu 2000). The assumption that the threshold pressure had to be higher for stem tissues than for young tissues or individual cells on which most of the

measurements had been made, led to the choice of $\Gamma = 0.9$ MPa (Génard et al. 2001). Parameter ε_0 was given an arbitrary value of 1100 so that the simulated values of the elastic modulus ε (Equation 20) ranged between 12 to 20 MPa. These estimates are within the range of the values obtained for giant algal cells (from 10 to 60 MPa) and higher plant tissues (from 0 to 30 MPa) as reported by Dainty (1976), Tyree and Jarvis (1982), Dale and Sutcliffe (1986) and Larcher (2003). The length of the stem was measured at the beginning of the experiment (1 m) and used as initial *l*.

Integration of the model equations also requires initial values to be specified for D, D_i, d^s, Ψ_p^s, W(stem) and W(crown). We measured D with a sliding calliper (D = 0.0176 m) at the location of the LVDT. Initial values for D_i and d^s were then calculated by Equations 15 and 18, respectively. Following the approach of Génard et al. (2001), the initial value for the pressure potential in the stem storage compartment was approximated from data acquired during the night preceding collection of the data set used for simulation. Under these conditions, the pressure potential in the stem storage compartment can be assumed proportional to the water potential of the stem xylem (Fanjul and Rosher 1984):

$$\Psi_p^s = \beta\left(\Psi_{t=0}^x - \Psi^x(\Psi_p^s = 0)\right) \text{ for the stem at } t = 0 \qquad (44)$$

where β is an empirical parameter estimated during the calibration procedure; and $\Psi^x(\Psi_p^s = 0)$ is the water potential of the stem xylem for which the zero pressure potential in the storage compartment is reached. Following the approach of Génard et al. (2001), the value of –2.9 MPa given by Fanjul and Rosher (1984) for apple leaves under well-watered conditions was used for $\Psi^x(\Psi_p^s = 0)$. For $\Psi_{t=0}^x$(stem), the value of $\Psi_{t=0}^x$(roots) was used, which was estimated from soil water potential data measured during the night. The initial value for the stem storage water content W_0(stem) (i.e., 24,000 mg) was calculated from the geometry of the stem (Equation 17), taking into account that only 40% of the total stem storage volume V^s consists of water. The initial value of the crown storage water content W_0(crown) (i.e., 14,000 mg) was calculated from measurements of fresh mass and dry mass of the branches after the experiments on the young tree were finished.

Model simulation and calibration

For simulations with both HydGro and RCGro, a fourth-order Runge-Kutta numerical integrator with variable step size was used (integrator settings: accuracy = 1×10^{-6} and maximum step size = 0.1). For model calibration the simplex method, which is one of the search algorithms implemented in WEST and originally developed by Nelder and Mead (1965), was used to minimize the weighted sum of squared errors for the variables F(stem) and D. The weights used to account for the differences in the order of magnitude for both variables in the objective function were based on the inverse of the variance of the measurement errors (Dochain and Vanrolleghem 2001).

The success of the parameter estimation process was evaluated by checking the quality of the parameters based on the parameter estimation error covariance matrix. Based on this matrix, the standard errors of the parameters can be calculated as $\sigma(\theta_i) = \sqrt{V_{ii}}$ where V_{ii} is an element on the diagonal of the covariance matrix. Confidence intervals for the parameters are then obtained as:

$$\theta \pm t_{\alpha;N-p}\sigma(\theta_i) \qquad (45)$$

for a confidence level specified as $100(1 - \alpha)$% where t is the value obtained from the two-tailed Student-t distribution and N is total number of measurements used to estimate the p parameters.

Objective model selection methodology

An objective model selection criterion called the Final Prediction Error (FPE) was used to select the better model (i.e., HydGro or RCGro) and, consequently, the better approach to calculate the capacitance of storage tissues. We calculated FPE as (Dochain and Vanrolleghem 2001):

$$\text{FPE} = \frac{\text{SSR}}{N} + \frac{2p\text{SSR}}{(N - p)N} \qquad (46)$$

where SSR is the weighted sum of squared residuals for F(stem) and D, N is number of measurements and p is the number of estimated parameters. The first term positively evaluates a better fit of the model to the data and the second term penalizes over-parameterized models. Thus, the smallest criterion value reveals the better model.

Results

Model calibration

For calibration of both HydGro and RCGro, experimental data with distinct sap flow dynamics and fast stem diameter growth were used. Figure 6 shows the daily fluctuation of the microclimate imposed on the young beech tree in the growth room, together with E. The fluctuating course of E during the second half of the daytime period (Figure 6d) was mainly driven by the fluctuating course of the vapor pressure deficit of the air (Figure 6c). This resulted from the slow response time and hysteresis of the temperature controller in the growth room (fluctuation of about 0.4 °C around the selected air temperature of 23 °C, Figure 6b).

HydGro and RCGro were calibrated, with E as the input variable, by minimizing the weighted squared difference between the model output and the measured data for F(stem) and D. The estimated parameters, together with their $(t_{\alpha;N-p})(\sigma(\theta))$ values (for the 95% confidence interval, Equation 45) and their error percentages, are listed in Table 3.

The estimated parameters resulted in model outputs that fitted the experimental data well. Figure 7 illustrates the model fits for F(stem) and D using HydGro and RCGro. Although HydGro and RCGro apparently generate outputs that are simi-

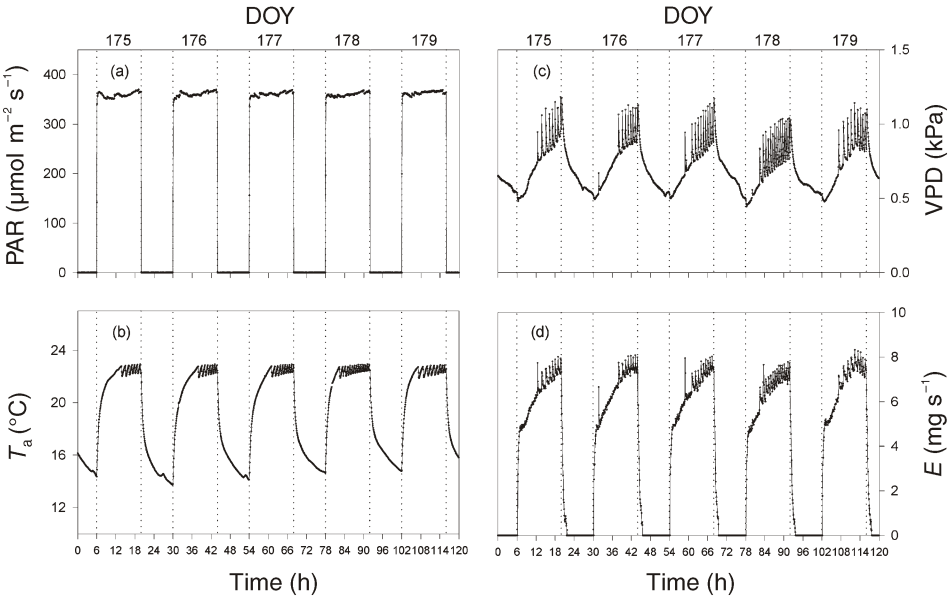

Figure 6. A 5-day sample (day of year DOY 175–179) of the varying microclimate in the growth room: (a) photosynthetically active radiation (PAR), (b) air temperature (T_a) and (c) vapor pressure deficit (VPD); and of (d) leaf transpiration rate (E). Transpiration rate is used as input for calibration of both HydGro and RCGro for a young beech tree. Vertical dotted lines correspond to the beginning and end of the daylight period. Daytime oscillations were caused by the slow response and hysteresis of the temperature controller in the growth room.

lar, differences were observed (e.g., the differences indicated in Figures 7I–7IV). Compared with F(stem) computed with RCGro, F(stem) computed with HydGro reaches zero more slowly at the beginning of each night (Figure 7I versus 7III). Also, RCGro computes a slow decrease in D during the day, whereas HydGro simulates a rather horizontal D course (cf. Figure 7II and 7IV). To explain these differences, the respective desorption curves (Figure 8) were reconstructed from simulated time courses of the total water potential and the water content in the storage compartments. For HydGro, the theoretical desorption curve was calculated using the calibrated model parameters k_1(pool) and k_2(pool) (see Model description). From the inverse slopes of the desorption curves, the time courses of the capacitances were calculated (Figure 9). Differences in capacitance C were revealed: C for both stem and crown obtained from HydGro are much larger during the night compared with the values obtained from RCGro.

To select the better model for predicting sap flow dynamics and stem diameter variation, scatter plots were produced to compare simulated data with measured data (Figure 10) and the objective model selection criterion FPE calculated. For the calibration data set, FPE was 0.1566 and 0.1501 for HydGro and RCGro, respectively, and the corresponding values for the validation data set were 0.5252 and 0.3851.

Model validation

The quality and reliability of the calibrated models were further assessed by a validation step with another subset of experimental data that included physiological responses of the tree (Figure 11) to step changes in PAR imposed on DOY 184 and 185 (Figure 11a). During both days, PAR was suddenly decreased from 360 to 55 µmol m^{-2} s^{-1} at 1300 h; however, the low PAR was maintained during the remainder of DOY 184, whereas it was increased at 1825 h on DOY 185. As shown in Figure 11b, the step changes in PAR also had effects on air temperature and, thus, vapor pressure deficit (Figure 11c) and E (Figure 11d).

Together with the parameter estimates reported in Table 3, E

Table 3. Estimated parameter values of HydGro and RCGro for a young beech tree between day of year 175 and 179. The values of $(t_{\alpha;N-p})(\sigma(\theta))$ used to compute the 95% confidence interval (Equation 45) and the error percentage (error %) are also given. The error percentage is defined as the ratio of $(t_{\alpha;N-p})(\sigma(\theta))$ and the respective estimated parameter value. See Table 2 for units and definitions of the parameters.

HydGro				RCGro			
Parameter	Value	$(t_{\alpha;N-p})(\sigma(\theta))$	Error %	Parameter	Value	$(t_{\alpha;N-p})(\sigma(\theta))$	Error %
k_1(stem)	23733.0	1.9	0.01	C(stem)	212.3	0.5	0.22
k_2(stem)	54.4	0.9	1.73	C(crown)	1157.6	100.4	8.67
k_1(crown)	11684.4	159.7	1.37				
k_2(crown)	563.3	32.2	5.72				
R^x	0.1853	0.0081	4.40	R^x	0.1829	0.0005	0.27
β	0.3385	0.0003	0.10	β	0.3385	0.0002	0.05
ϕ	2.35×10^{-7}	7.94×10^{-10}	0.34	ϕ	2.34×10^{-7}	2.83×10^{-9}	1.21
L	1.12×10^{-7}	2.60×10^{-8}	23.25	L	8.38×10^{-8}	2.76×10^{-8}	32.96

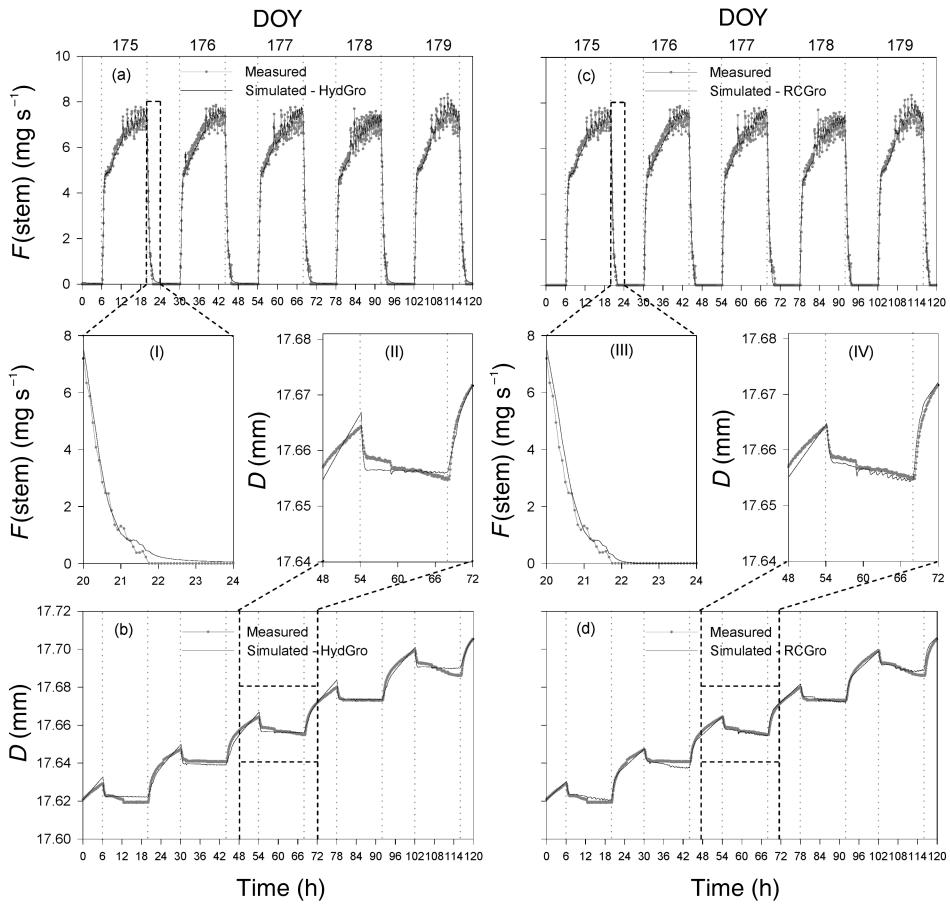

Figure 7. Model calibration (day of year (DOY) 175–179) showing comparisons between measured and simulated sap flow rate (F(stem)) at stem base (a and c) and between the measured and simulated diameter variation (D) of the stem (b and d) for HydGro (a and b) and RCGro (c and d). Measured data were obtained every 5 min. Vertical dotted lines represent the beginning and end of the daylight period. Details of simulation results are also shown (I–IV) to illustrate specific differences between model outputs obtained with HydGro and RCGro.

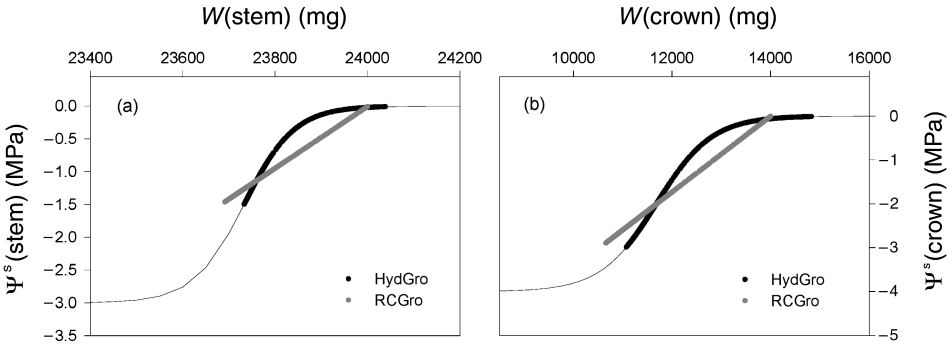

Figure 8. Desorption curves for the stem (a) and the crown (b) storage pool of a young beech tree. The thin line represents the entire desorption curve obtained from the HydGro model after calibration (Equation 12), and symbols (black circles) indicate the part of the curve that was used during simulation. The straight gray line represents the desorption curve used during model simulation with RCGro.

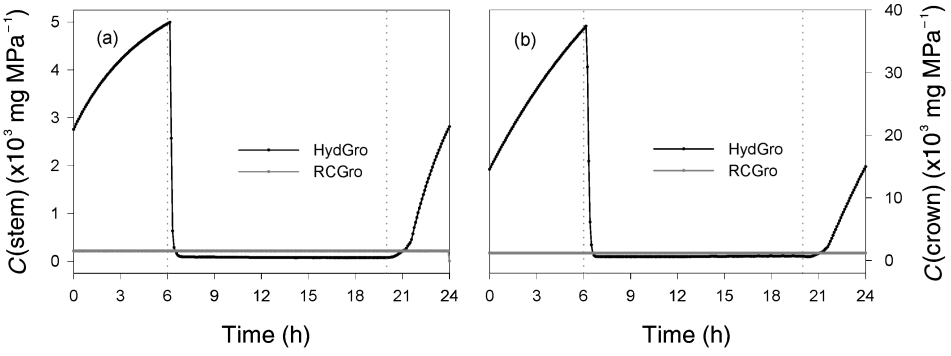

Figure 9. Diurnal courses of hydraulic capacitance C for the stem (a) and the crown (b) storage pool of a young beech tree. Capacitance values were derived from the inverse of the slopes of the desorption curves presented in Figure 8. A distinction is made between C values used by HydGro and by RCGro. Vertical dotted lines represent the beginning and end of the daylight period.

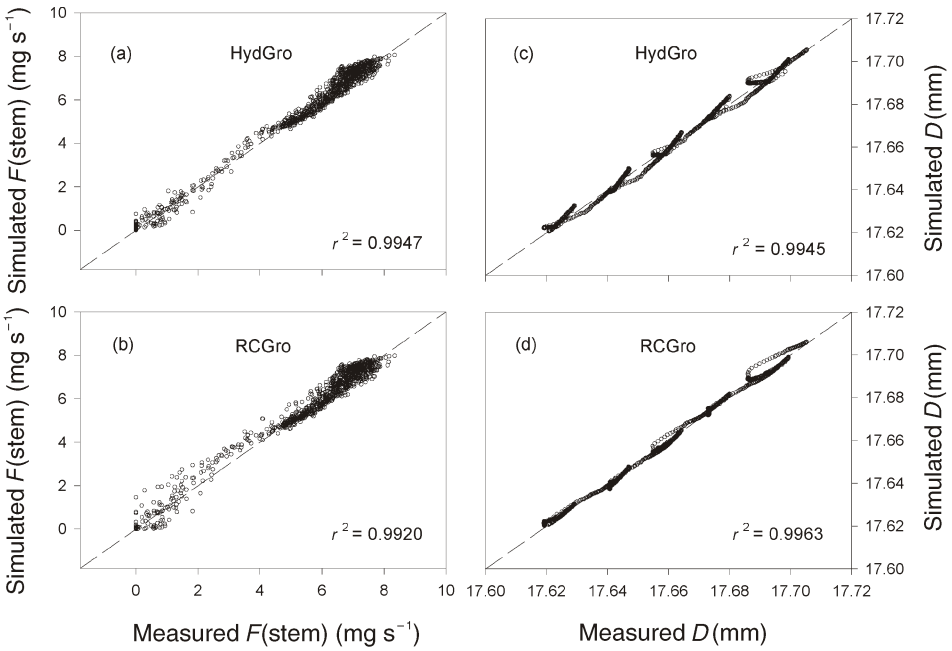

Figure 10. Scatter plots of measured and simulated data (day of year (DOY) 175–179) for sap flow rate at the stem base F(stem) and stem diameter variation D, obtained with HydGro (a, c) and RCGro (b, d). Dashed line represents the 1:1 relationship. Coefficients of determination (r^2) are given.

was used to test the validity of both models. Without additional calibration, good agreement was found between model simulations for sap flow and stem diameter variation and measurements (Figure 12).

Discussion

Performance of the flow and storage model

Both the HydGro and RCGro approach of the flow and storage model successfully simulate sap flow dynamics and stem diameter variation of the young beech tree (Figures 7 and 12). In contrast to existing models (e.g., Perämäki et al. 2001, Zweifel et al. 2001), the simulated change in stem diameter also included stem growth, which is superimposed on the daily diameter fluctuation driven by changes in internal water storage. This model extension appears to be essential to obtain good simulation results and it helps to explore the mechanisms underlying stem growth. Stem growth of the young beech tree occurred mainly during the night when the pressure potential in the stem storage compartment exceeded the wall-yielding threshold value Γ (Figure 13), indicating that stem growth is a highly dynamic process. To reveal the daily fluctuation in stem diameter caused by changes in water storage, Sevanto et al. (2002) subtracted a linear trend line for growth from the original measured stem diameter variations. For the beech tree, use

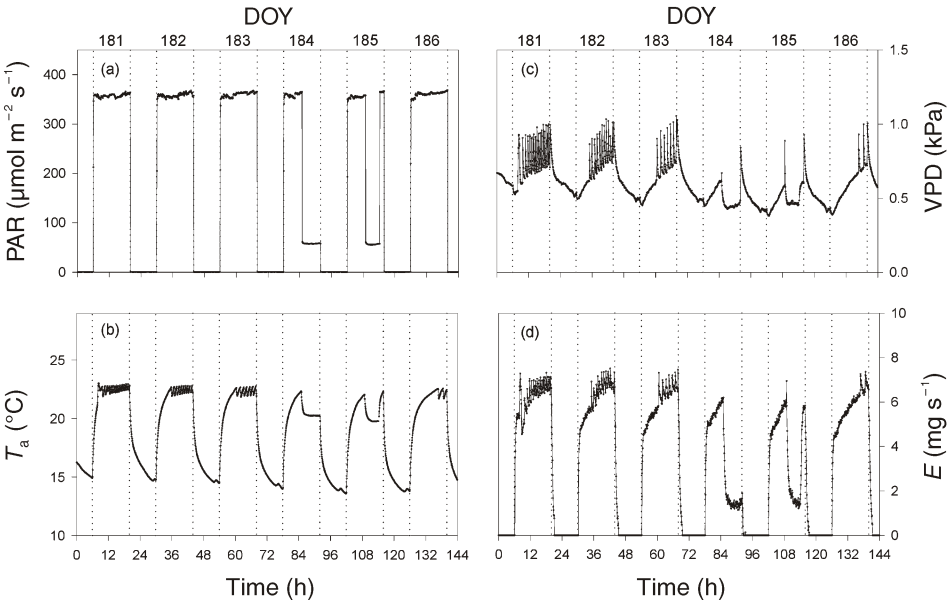

Figure 11. A 6-day sample (day of year (DOY) 181–186) of the varying microclimate in the growth room: (a) photosynthetically active radiation (PAR), (b) air temperature (T_a) and (c) vapor pressure deficit (VPD); and (d) the leaf transpiration rate (E). Transpiration rate is used as input for validation of the calibrated HydGro and RCGro model for a young beech tree. Vertical dotted lines correspond to the beginning and end of the daylight period. A step change in PAR was made on DOY 184 and 185.

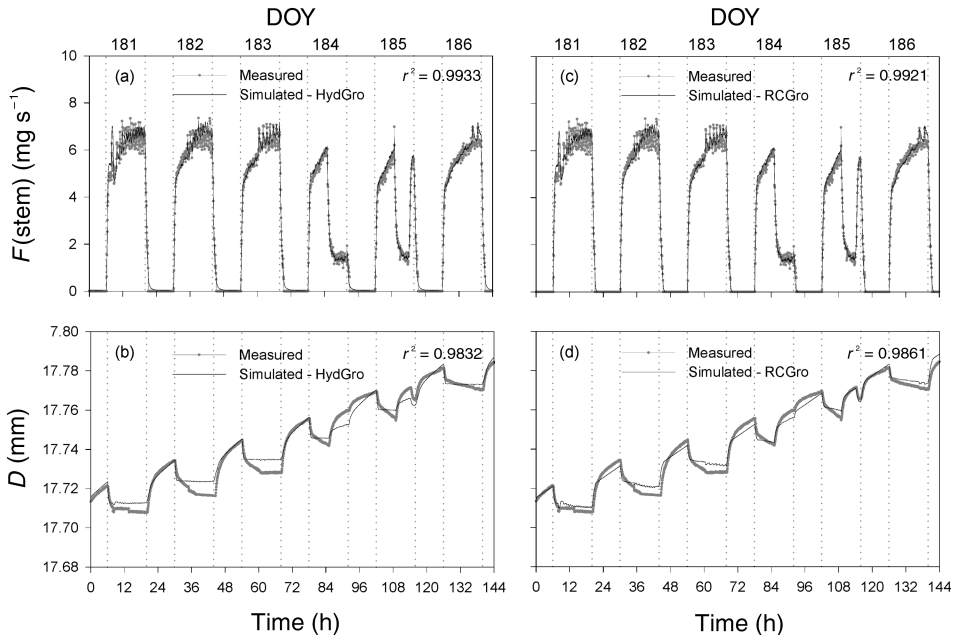

Figure 12. Validation of the calibrated models (day of year (DOY) 181–186) showing the comparison between measured and simulated sap flow rate (F(stem)) at stem base (a, c) and between measured and simulated stem diameter variation (D) (b, d) for HydGro (a, b) and RCGro (c, d). Measured data were obtained every 5 min. Vertical dotted lines represent the beginning and end of the daylight period. Coefficients of determination (r^2) are given.

of this procedure in Figures 7 or 12 is invalid because it would lead to stem diameters that continuously shrink during the daytime, whereas, in reality, stem diameter is constant during periods of steady-state water flow.

The model assumption that daily fluctuations in stem diameter driven by changes in stem water storage take place in the tissue external to the xylem because the water content of the xylem is constant under the experimental conditions imposed is reasonable for the following reasons. Several authors have reported that daily stem diameter fluctuations occur mainly in the elastic tissues of the bark, whereas the xylem of the stem undergoes only small fluctuations (Dobbs and Scott 1971, Molz and Klepper 1973, Brough et al. 1986, Zweifel et al. 2000). At least 75% of the observed diameter changes could be attributed to the extensible tissues external to the mature xylem. Measurements of xylem and whole-stem (over-bark) diameter variations of the young beech tree indicate that more than 80% of the stem diameter fluctuation occurred in the bark (Steppe 2004). The larger fluctuations in whole-stem diameter compared with xylem diameter also indicate that xylem is a more rigid material. More importantly, the larger amplitude of the whole-stem diameter variations results from water exchange between the xylem and the outer tissue. Thus, it is justified to consider the bark as an important pool of internally stored water in the stem. Furthermore, it is possible to estimate rates of water depletion and replenishment in the bark from continuous measurements of the whole stem (Zweifel and Häsler 2001). Based on large time lags (30 to 110 min) between whole-stem and xylem diameter variations for Scots pine trees, Sevanto et al. (2002, 2003) related the diameter variations and the observed time lags to the transport of carbohydrates in the phloem and concluded that phloem and bark did not represent a significant water storage pool. However, the absence of a time lag between whole-stem and xylem diameter variations in the young beech tree (Steppe 2004) and the strong linear relationship between rate of change in water storage and rate of change in stem diameter (Steppe and Lemeur 2004) strongly suggest that water stored in the phloem and bark is hydraulically connected to the water in the xylem and that the hydraulic conductivity between the internal stem storage pool and the transpiration stream is high.

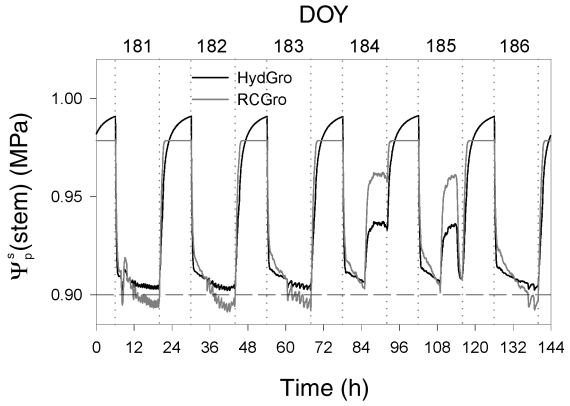

Figure 13. Comparison of simulations for the pressure potential in the stem storage compartment ($\Psi^s_{p\,(stem)}$) obtained with HydGro and RCGro (day of year (DOY) 181–186). Vertical dotted lines represent the beginning and end of the daylight period. The horizontal dashed line represents the wall-yielding threshold pressure Γ.

The strong stem diameter response to changes in sap flow is of considerable physiological interest. When E, and subsequently F(stem) suddenly decreased in response to an imposed step change in PAR, a sharp increase in stem diameter D was observed (Figures 12b and 12d; DOY 184 and 185). Model simulations indicate that the increase in D is partly a result of refilling of the internal stem storage pool in addition to stem

growth. Thus, growth is driven by the increase in pressure potential as shown in Figure 13. This particular effect emphasizes the importance of including growth in water flow models for establishing the correct link between sap flow dynamics and stem diameter variation.

Quality assessment of estimated parameters is an essential part of model calibration and so particular attention was given to the accuracy of the estimated parameters (Table 3). The parameters related to the capacitance of the stem storage pool (C(stem), k_1(stem), k_2(stem)) were estimated more precisely than those of the crown pool—as indicated by the lower error percentages of the former—because stem diameter variation was used for optimization, whereas no calibration was done for crown data. In the case of RCGro, the values for C were directly available, whereas for HydGro a desorption curve had to be generated to compute C. Comparison with C values from the literature is difficult because there is little agreement about the units for capacitance (Aumann and Ford 2002). Values with the same units that we used are reported to range from 1400 to 19,000 mg MPa^{-1} for leaves and from 1100 to 2,100,000 mg MPa^{-1} for stems (Milne and Young 1985, Wronski et al. 1985, Hunt et al. 1991, Kobayashi and Tanaka 2001, Lhomme et al. 2001). Compared with these values, the capacitance values estimated for the young beech tree are low, probably because all published values were obtained for adult trees and tree species other than *Fagus sylvatica*. For the hydraulic parameter R^x, the estimates were almost identical using either HydGro or RCGro; the difference being that the value could be estimated more accurately with RCGro (Table 3). The estimated resistance was higher than reported literature values, reflecting the small vessel diameters of the xylem of the young beech tree (Steppe et al. 2004). For example, values of hydraulic resistance ranging from 0.003 to 0.006 MPa s mg^{-1} have been reported for *Fagus sylvatica* (Magnani and Borghetti 1995), values ranging from 0.012 to 0.024 MPa s mg^{-1} for *Quercus Pubescens* (Tognetti et al. 1998), a value of 0.0063 MPa s mg^{-1} for *Picea sitchensis* (Milne and Young 1985) and a value of 0.1 MPa s mg^{-1} for *Malus pumila* (Landsberg et al. 1976).

Among the model parameters related to growth, the empirical dimensionless parameter β could be estimated accurately (low error percentages and small confidence intervals for both approaches). The ϕ value for bark tissue of the young beech tree was 2.35×10^{-7} MPa^{-1} s^{-1}. Cell wall extensibility usually ranges from 8.33×10^{-6} to 5.56×10^{-5} MPa^{-1} s^{-1} (Hsiao et al. 1998), which is an order of magnitude higher than the value estimated for the beech tree, probably because ϕ is usually measured on young and extensible leaf tissues. Génard et al. (2001) also found a high extensibility ($\phi = 3.19 \times 10^{-7}$ MPa^{-1} s^{-1}) for plum roots and attributed this to the fact that the roots were 5 years old.

Radial hydraulic conductivity L was estimated to fall within the 95% confidence interval from 8.60×10^{-8} to 1.38×10^{-7} m MPa^{-1} s^{-1} for HydGro and from 5.62×10^{-8} to 1.11×10^{-7} m MPa^{-1} s^{-1} for RCGro, which is in the range reported for giant algal cells (from 1.86×10^{-8} to 2.78×10^{-4} m MPa^{-1} s^{-1}) and for cells of higher plants (from 1.0×10^{-10} to 1.67×10^{-4} m MPa^{-1} s^{-1}) (Dainty 1976, Dale and Sutcliffe 1986, Génard et al. 2001). The absolute values of this parameter should be used with care, however, because the error percentages calculated for L are large—a manifestation of the lower sensitivity of L which makes it more difficult to estimate.

The time frame that the flow and storage model uses to predict stem diameter variations is between a day and 2 weeks. A longer time frame resulted in poorer predictions of stem diameter variations because of the time dependency of some of the model parameters (Steppe 2004). Although the model was applied to a young beech tree, there is no restriction concerning its application to other tree species.

Desorption curve and capacitance

Differences in model outputs between HydGro and RCGro (Figure 7) are attributable to the different methods of calculating C of the storage tissue. Typical time courses of C are shown in Figure 9. The higher nighttime C values of HydGro compared with RCGro imply that more water can be stored (per unit pressure drop) in the storage pools of the stem and the crown at less negative water potentials. The physiological meaning of this observation is revealed by considering the nature of the desorption curve used by HydGro (Figure 8). The curve consists of two parts: a part from 0 to –0.3 MPa where there is a rather large C and a part below –0.5 MPa where C is small. The first part refers to capillary water stored in intercellular spaces; whereas the second part represents the elastic storage in cells of the bark and the cambium. Such phases in desorption phenomena have been extensively discussed by Tyree and Yang (1990) and Tyree and Zimmermann (2002). In addition, these authors indicate a third part in the desorption curve where C is again high at very negative water potentials, because of the release of stored water by cavitation. In the young beech tree, the contribution of stored water released by cavitation could be neglected.

During daytime, both models use a constant storage capacitance; the capacitance of HydGro being somewhat lower than that of RCGro because of the steeper slope of the straight line interconnecting the Ψ^s(pool) values of less than –0.3 MPa. Hunt et al. (1991) noted that constant plant capacitances for modeling the diurnal water flow in plants can be obtained from bended desorption curves (i.e., omitting the initial part (capillary stored water) of the pressure–volume curve). According to Hunt et al. (1991), the slope of the remaining curve then approximates a constant value that can be used in plant models. However, Figure 9 illustrates that C values obtained in this way would be lower than the C values that were obtained through model calibration of RCGro (represented by the straight lines in Figure 8), indicating that care should be taken when trying to deduce constant capacitances from bended desorption curves.

Model selection

Both HydGro and RCGro predict sap flow dynamics in a realistic way and describe well the variation in stem diameter. The

results of model calibration were good and both models successfully passed the model validation procedure, confirming that the processes driving both model approaches are adequate and describe the underlying physiological mechanisms correctly. The choice between use of variable or fixed capacitances in the flow and storage model cannot be made based on r^2 values (Figures 10 and 12) because both models have a similar predicting power for F(stem) and D; however, FPE values show that RCGro is the better model. No bended (complex) desorption curves are needed to calculate C of storage tissues. Additionally, models including only constant C values are less complex because there are fewer parameters to estimate.

In conclusion, existing models for simulating sap flow dynamics and stem diameter changes observed in individual trees are incomplete because they include only diameter fluctuations driven by changes in stem water storage. Inclusion of a stem growth component in the stem diameter variation is essential to obtain accurate simulations of F(stem) and D. Use of a bended curve (HydGro) or a straight line (RCGro) for the desorption curve to calculate C of storage tissues results in specific differences between the simulated variables. Based on sensitivity analysis, a subset of parameters could be identified driving most of the variability in the model outputs for F(stem) and D. This selection resulted in calibrated parameters with low error percentages and small confidence intervals. Good results for model calibration were obtained and both HydGro and RCGro successfully passed the validation procedure. Based on "Final Prediction Error" as the model selection criterion, RCGro is the better model, which also implies that the use of constant C resulted in better model simulations. We conclude that the flow and storage model is a powerful tool for detailed and fundamental analyses of sap flow dynamics and stem diameter variation. The model also allows accurate assessment of physiological characteristics that are difficult to measure (e.g., hydraulic resistance, hydraulic capacitance and cell wall extensibility).

Acknowledgments

This paper reports on parts of the Ph.D. study undertaken by Kathy Steppe. The authors thank the Flemish Fund for Scientific Research (F.W.O.-Vlaanderen) (Belgium) for providing the Ph.D. funding. They are also indebted to Philip Deman, technician of the Laboratory of Plant Ecology, for his enthusiastic support and highly valuable contribution to the experimental set-up.

References

Aumann, C.A. and E.D. Ford. 2002. Modeling tree water flow as an unsaturated flow through a porous medium. J. Theor. Biol. 219: 415–429.

Bradford, K.J. and T.C. Hsiao. 1982. Physiological responses to moderate water stress. *In* Encyclopedia of plant physiology, New Series. Eds. O.L. Lange, P.S. Nobel, C.B. Osmond and H. Ziegler. Springer-Verlag, Berlin, pp 263–324.

Bréda, N., H. Cochard, E. Dreyer and A. Granier. 1993. Field comparison of transpiration, stomatal conductance and vulnerability to cavitation of *Quercus petraea* and *Quercus robur* under water stress. Ann. Sci. For. 50:571–582.

Brough, D.W., H.G. Jones and J. Grace. 1986. Diurnal changes in water content of the stem of apple-trees as influenced by irrigation. Plant Cell Environ. 9:1–7.

Brun, R., M. Kühni, H. Siegrist, W. Gujer and P. Reichert. 2002. Practical identifiability of ASM2d parameters: systematic selection and tuning of parameter subsets. Water Res. 36:4113–4127.

Cochard, H., N. Bréda and A. Granier. 1996. Whole tree hydraulic conductance and water loss regulation in *Quercus* during drought: evidence for stomatal control of embolism? Ann. Sci. For. 53: 197–206.

Cochard, H., D. Lemoine and E. Dreyer. 1999. The effect of acclimation to sunlight on the xylem vulnerability to embolism in *Fagus sylvatica* L. Plant Cell Environ. 22:101–108.

Dainty, J. 1976. Water relations of plant cells. *In* Encyclopaedia of Plant Physiology. New Series, Vol 2A. Eds. U. Lüttge and M.G. Pitman. Springer-Verlag, Berlin, pp 12–35.

Dale, J.E. and J.F. Sutcliffe. 1986. Water relations of plant cells. *In* Plant Physiology—Water and Solutes in Plants. Vol 9. Ed. F.C. Steward. Academic Press, Orlando, pp 1–48.

Dobbs, R.C. and D.M.R. Scott. 1971. Distribution of diurnal fluctuations in stem circumference of Douglas-fir. Can. J. For. Res. 1: 80–83.

Dochain, D. and P.A. Vanrolleghem. 2001. Dynamical modelling and estimation in wastewater treatment processes. IWA Publishing, London, 360 p.

Edwards, W.R.N., P.G. Jarvis, J.J. Landsberg and H. Talbot. 1986. A dynamic model for studying flow of water in single trees. Tree Physiol. 1:309–324.

Fanjul, L. and P.H. Rosher. 1984. Effects of water stress on internal water relations of apple leaves. Physiol. Plant. 62:321–328.

Génard, M., S. Fishman, G. Vercambre, J.-G. Huguet, C. Bussi, J. Besset and R. Habib. 2001. A biophysical analysis of stem and root diameter variations in woody plants. Plant Physiol. 126: 188–202.

Goldstein, G., J.L. Andrade, F.C. Meinzer, N.M. Holbrook, J. Cavelier, P. Jackson and A. Celis. 1998. Stem water storage and diurnal patterns of water use in tropical forest canopy trees. Plant Cell Environ. 21:397–406.

Green, P.B. and W.R. Cummins. 1974. Growth rate and turgor pressure: auxin effect studied with an automated apparatus for single coleoptiles. Plant Physiol. 54:863–869.

Green, P.B., R.O. Erickson and J. Buggy. 1971. Metabolic and physical control of cell elongation rate: in vivo studies in *Nitella*. Plant Physiol. 47:423–430.

Grime, V.L., J.I.L. Morison and L.P. Simmonds. 1995. Including the heat storage term in sap flow measurements with the stem heat balance method. Agric. For. Meteorol. 74:1–25.

Herzog, K.M., R. Häsler and R. Thum. 1995. Diurnal changes in the radius of a subalpine Norway spruce stem: their relation to the sap flow and their use to estimate transpiration. Trees 10:94–101.

Hsiao, T.C., J. Frensch and B.A. Rojas-Lara. 1998. The pressure-jump technique shows maize leaf growth to be enhanced by increases in turgor only when water status is not too high. Plant Cell Environ. 21:33–42.

Hsiao, T.C. and L.-K. Xu. 2000. Sensitivity of growth of roots versus leaves to water stress: biophysical analysis and relation to water transport. J. Exp. Bot. 51:1595–1616.

Huguet, J.G. 1985. Appréciation de l'état hydrique d'une plante à partir des variations micrométriques de la dimension des fruits ou des tiges au cours de la journée. Agronomie 5:733–741.

Hunt, E.R., Jr., S.W. Running and C.A. Federer. 1991. Extrapolating plant water flow resistances and capacitances to regional scales. Agric. For. Meteorol. 54:169–195.

Jarvis, P.G., W.R.N. Edwards and H. Talbot. 1981. Models of plant and crop water use. *In* Mathematics and Plant Physiology. Eds. D.A. Rose and D.A. Charles-Edwards. Academic Press, London, pp 151–194.

Jones, H.G. 1992. Plants and microclimate. A quantitative approach to environmental plant physiology. University Press, Cambridge, 428 p.

Katchalsky, A. and P.F. Curran. 1965. Nonequilibrium thermodynamics in biophysics. Harvard University Press, Cambridge, 248 p.

Kobayashi, Y. and T. Tanaka. 2001. Water flow and hydraulic characteristics of Japanese red pine and oak trees. Hydrol. Process. 15:1731–1750.

Lambers, H., F.S. Chapin III and T.L. Pons. 1998. Plant physiological ecology. Springer-Verlag, New York, 540 p.

Landsberg, J.J., T.W. Blanchard and B. Warrit. 1976. Studies on the movement of water through apple trees. J. Exp. Bot. 27:579–596.

Larcher, W. 2003. Physiological plant ecology. Ecophysiology and stress physiology of functional groups. Springer-Verlag, Berlin, 513 p.

Lhomme, J.P., A. Rocheteau, J.M. Ourcival and S. Rambal. 2001. Non-steady-state modelling of water transfer in a Mediterranean evergreen canopy. Agric. For. Meteorol. 108:67–83.

Lockhart, J.A. 1965. An analysis of irreversible plant cell elongation. J. Theor. Biol. 8:264–275.

Magnani, F. and M. Borghetti. 1995. Interpretation of seasonal changes of xylem embolism and plant hydraulic resistance in *Fagus sylvatica*. Plant Cell Environ. 18: 689–696.

Milne, R. and P. Young. 1985. Modelling of water movement in trees. IFAC Identification and System Parameter Estimation. Proc. 7th IFAC/IFORS Symp. 463–468.

Molz, F.J. and B. Klepper. 1973. On the mechanism of water-stress-induced stem deformation. Agron. J. 65:304–306.

Nelder, J.A. and R. Mead. 1965. A simplex method for function minimization. Computer J. 7:308–313.

Nobel, P.S. 1999. Physicochemical and environmental plant physiology. Academic Press, San Diego, 474 p.

Perämäki, M., E. Nikinmaa, S. Sevanto, H. Ilvesniemi, E. Siivola, P. Hari and T. Vesala. 2001. Tree stem diameter variations and transpiration in Scots pine: an analysis using a dynamic sap flow model. Tree Physiol. 21:889–897.

Raftoyannis, Y and K. Radoglou. 2002. Physiological responses of beech and sessile oak in a natural mixed stand during a dry summer. Ann. Bot. 89:723–730.

Schulze, E.-D., J. Èermák, R. Matyssek, M. Penka, R. Zimmermann, F. Vasicek, W. Gries and J. Kuèera. 1985. Canopy transpiration and water fluxes in the xylem of the trunk of *Larix* and *Picea* trees—a comparison of xylem flow, porometer and cuvette measurements. Oecologia 66:475–486.

Sevanto, S., T. Vesala, M. Perämäki and E. Nikinmaa. 2002. Time lags for xylem and stem diameter variations in a Scots pine tree. Plant Cell Environ. 25:1071–1077.

Sevanto S., T. Vesala, M. Perämäki and E. Nikinmaa. 2003. Sugar transport together with environmental conditions controls time lags between xylem and stem diameter changes. Plant Cell Environ. 26:1257–1265.

Simonneau, T., R. Habib, J.-P. Goutouly and J.-G. Huguet. 1993. Diurnal changes in stem diameter depend upon variations in water content: direct evidence in peach trees. J. Exp. Bot. 44:615–621.

Steppe, K. 2004. Diurnal dynamics of water flow through trees: design and validation of a mathematical flow and storage model. Doctoral thesis, Ghent University, Belgium, 272 p.

Steppe, K., V. Cnudde, C. Girard, R. Lemeur, J.-P. Cnudde and P. Jacobs. 2004. Use of X-ray computed microtomography for non-invasive determination of wood anatomical characteristics. J. Struct. Biol. 148:11–21.

Steppe, K. and R. Lemeur. 2004. An experimental system for analysis of the dynamic sap-flow characteristic in young trees: results of a beech tree. Funct. Plant Biol. 31:83–92.

Steppe, K., R. Lemeur and R. Samson. 2002. Sap flow dynamics of a beech tree during the solar eclipse of 11 August 1999. Agric. For. Meteorol. 112:139–149.

Steudle, E. 2000. Water uptake by roots: effects of water deficit. J. Exp. Bot. 51:1531–1542.

Tatarinov, F. and J. Cermak. 1999. Daily and seasonal variation of stem radius in oak. Ann. For. Sci. 56:579–590.

Tognetti, R., A. Longobucco and A. Raschi. 1998. Vulnerability of xylem to embolism in relation to plant hydraulic resistance in *Quercus pubescens* and *Quercus ilex* co-occurring in a Mediterranean coppice stand in central Italy. New Phytol. 139:437–447.

Tyree, M.T. 1988. A dynamic model for water flow in a single tree: evidence that models must account for hydraulic architecture. Tree Physiol. 4:195–217.

Tyree, M.T. and P.G. Jarvis. 1982. Water in tissues and cells. *In* Encyclopedia of Plant Physiology. New Series. Eds. O.L. Lange, P.S. Nobel, C.B. Osmond and H. Ziegler. Springer-Verlag, Berlin, pp 35–77.

Tyree, M.T. and S. Yang. 1990. Water-storage capacity of *Thuja*, *Tsuga* and *Acer* stems measured by dehydration isotherms. Planta 182:420–426.

Tyree, M.T. and M.H. Zimmermann. 2002. Xylem structure and the ascent of sap. Springer-Verlag, Berlin, 283 p.

van Bavel, M.G. and C.H.M. van Bavel. 1990. Dynagage installation and operational manual. Dynamax, Houston, TX, 80 p.

van den Honert, T.H. 1948. Water transport in plants as a caternary process. Discuss. Faraday Soc. 3:146–153.

Vanhooren, H., J. Meirlaen, Y. Amerlinck, F. Claeys, H. Vangheluwe and P.A. Vanrolleghem. 2003. WEST: modelling biological wastewater treatment. J. Hydroinform. 5:27–50.

Wronski, E.B., J.W. Holmes and N.C. Turner. 1985. Phase and amplitude relations between transpiration, water potential and stem shrinkage. Plant Cell Environ. 8:613–622.

Zweifel, R. and R. Häsler. 2001. Dynamics of water storage in mature subalpine *Picea abies*: temporal and spatial patterns of change in stem radius. Tree Physiol. 21:561–569.

Zweifel, R., H. Item and R. Häsler. 2000. Stem radius changes and their relation to stored water in stems of young Norway spruce trees. Trees 15:50–75.

Zweifel, R., H. Item and R. Häsler. 2001. Link between diurnal stem radius changes and tree water relations. Tree Physiol. 21:869–877.